Effects of inter-nanocrystal distance on the photoluminescence and electrical properties of silicon nanocrystals

Author: Pablo Blasco Ladrero
*Facultat de Física, Uniersitat de Barcelona, Diagonal 645, 08028 Barcelona, Spain.**

Advisors: Dr. Julià López Vidrier and Dr. Sergi Hernández Márquez
(Dated: January 16, 2019)

Abstract: The effect of the variation of the distance between size-controlled silicon nanocrystals (Si NCs) on their electrical properties and low-temperature photoluminescence (PL) emission are studied in the present project. Via the superlattice approach, SiO_2 barrier thicknesses from 1 nm to 3 nm, with 0.5 nm steps, alternated with layers of silicon-rich oxynitride (SRON), were deposited on a *p*-type Si substrate through plasma-enhanced chemical-vapor deposition. After an adequate annealing process, the precipitation of Si NCs was achieved. The low-temperature PL data were fitted using a physical model which takes into account the electron-phonon interaction between NCs, from which the average phonon energy was estimated. The obtained results demonstrate that thicker barriers (i.e., higher inter-NC distance) present lower average phonon energy, which is ascribed to a weaker NC-NC interaction and a greater carrier confinement. In addition, the $I(V)$ from NCs-containing device were studied. High applied electric fields resulted in Fowler-Nordheim (F-N) mechanism dominating charge transport, from which the values of the band offset energy between the electrode and the NCs-containing dielectric were figured out, being this value larger for thicker barriers, in agreement with a lower injection efficiency.

I. INTRODUCTION

Silicon (Si) has been the most used semiconductor material in Electronics since the beginning of the field during the past century. The knowledge about this material, its abundance (it is the second most abundant element in the Earth crust) and ease of manipulation, has helped to maintain this privilege position inside the semiconductor materials world. However, bulk Si is not considered a good candidate for optical emission applications due to its indirect and near infrared (E_g=1.12 eV) band gap, which dramatically decreases the band-to-band electron transition probability.

In the last decades, the effect of quantum confinement in semiconductors has been widely studied, which is typically observable when one of the dimensions of the material under study is reduced to the nanometric scale. Once this condition is achieved, the energy states become discretized in the direction of the confinement and the energy band gap of the material is broadened. As a consequence, efficient light emission in the visible region of the electromagnetic spectrum has been observed in quantum-confined Si nanostructures [1], as well as the possibility to control the energy of the PL emission peak varying the nanostructure size. This fact increased the interest of the scientific community towards Si NCs, since it opened the possibility of efficiently employing the well-known Si within the field of Optoelectronics.

Because of the Si electronic properties dependence on the NC size, all efforts were focused on finding a technique that allows precisely controlling the size of the produced nanostructures. Different methods were developed but the most precise technique was proposed by M. Zacharias [2], the superlattice approach, which enables the precise control of the Si NCs size. This technique consists in the alternated deposition of a Si-rich Si-based dielectric and its stoichometric counterpart, followed by a high-temperature annealing treatment. Using this technique in the present bachelor thesis, and selecting silicon dioxide (SiO_2) as the Si-based dielectric, five samples with different thickness of the SiO_2 barrier have been synthetized. The modification of this parameter gives a more in-depth understanding on the effect of the inter-NC distance on their electronic properties.

The PL emission properties of Si NCs have been studied under low temperature conditions. The results obtained showed us that the conventional models used for the PL phenomena are no longer valid for the whole temperature range analysed, and Viña *et al.* correction must be used instead [3]. In addition, this expression allowed estimating the average phonon energy of the material system, which correlates to the confinement in the NCs.

Finally, the evolution of the electrical properties after modifying the SiO_2 barrier has also been investigated in terms of charge transport. The Fowler-Nordheim carrier transport mechanism (F-N) was found to dominate at high electric fields, and the injection efficiency was studied through the determination of the band offset energy at the interface between the metallic electrode and the SiO_2-embedded Si NCs.

*Electronic address: pblaslad@gmail.com

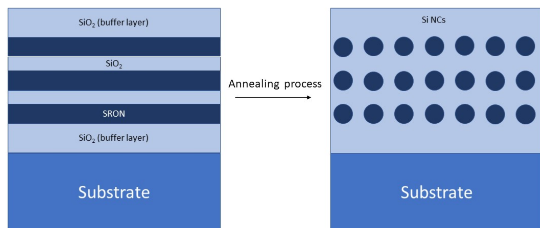

FIG. 1: Representation of the superlattice fabrication process, through the alternating deposition of SRON/SiO_2 bilayers on a certain substrate, in our case p-type Si. In addition, two thick layers of SiO_2 are deposited below and on top of the structure. After an annealing and passivation process the Si NCs are obtained.

II. EXPERIMENTAL DETAILS

A. Sample preparation

Samples containing twenty bilayers of silicon-rich silicon oxynitride (SRON) and stoichiometric SiO_2 were deposited on wet-chemically cleaned p-type Si substrates using plasma-enhanced chemical-vapor deposition (PECVD). A 10-nm-thick SiO_2 layer was additionally deposited both on top and below the superlattices as capping and buffer layer, respectively.

The thickness of the SiO_2 barriers was varied between 1 nm and 3 nm with steps of 0.5 nm between each sample. The SRON layer was kept with a constant thickness of 4 nm. The thickness of these layers was controlled knowing the deposition rate of the PECVD process for each material through ellipsometry characterization carried out on test samples. To induce the Si excess to precipitate and crystallize in the form of size-controlled Si NCs, all the samples were submitted to an annealing process in a quartz tube furnace at 1150 °C for 1 hour in a high-purity N_2 ambient. After this, the temperature was lowered down to 450 °C, the samples were passivated in H_2 rich medium for 1 h. FIG. 1 shows a schematics corresponding to the Si NCs superlattices fabrication process. Once the samples were fabricated, each of them was cut with a diamond tip into four equal pieces. Two of them were used for the PL measurements and the other two were further processed as devices for the electrical characterization. The remaining part was kept untouched as a control sample.

For the electrical characterization an additional fabrication process was performed to obtain a metal-insulator-semiconductor (MIS) structure where the insulator layer corresponds to the Si NC superlattices. A conventional photolithography process was carried out on the samples using a type of mask that allowed us to obtain three different sizes of circular aluminium contact. We varied the diameter of each contact having 0.5, 1 and 2 mm diameters. Both the top and the backside contacts of the Si-substrate were deposited with a thin film of aluminium by thermal evaporation.

B. Temperature-dependent PL characterization

Spectrally-resolved PL measurements were carried out by exciting the samples with the 325-nm line of a Kimmon HeCd continuous wave laser. The optical path was composed by mirrors that guided the beam light from the laser to the sample holder and focusing the beam onto the sample thanks to a convex lens, leading to a spot size of 80 μm in diameter. The power on the samples was controlled by using a pair of polarizers, leading to power densities of 22 $\mu W/cm^2$ and 54 $\mu W/cm^2$. Such low power densities have proved in the past to avoid excitonic oversaturation within the NCs [4]. In order to study the PL under low temperature, a single window CryoVac Konti cryostat chamber was placed on the sample holder. The window transmission coefficient was measured in orther to obtain the desired laser power on the samples. We could achieve high vacuum conditions inside the chamber ($P = 10^{-6}$ Pa) by using a regular vacuum pump connected in series to a turbomolecular pump. Low temperatures ranging from 4 K to 350 K were reached by filling the chamber with He, being the temperature measured through a thermocouple placed inside the chamber and the corresponding temperature controller. The PL spectra were analysed through Roper Scientific Acton optical Monochromator coupled to a highly-sensitive LN_2-cooled CCD camera.

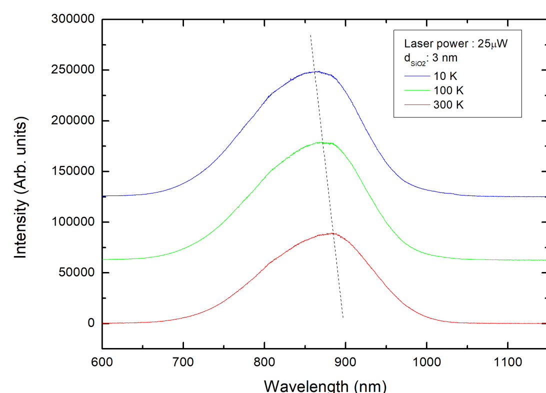

FIG. 2: Spectra obtained from the sample with 3-nm-thick SiO_2 barriers, under different temperatures, for 25 μW (54 $\mu W/cm^2$) power laser. As it can be seen in the plot, with the dashed line as an assistance, the peak emission shift toward shorter wavelengths (i.e., higher energies) at lower temperatures. This is what was expected, as semiconductors typically show a band gap broadening at lower temperatures.

To obtain the temperature-dependent PL, we started by cooling the samples down to 4 K and then increasing it using steps of 10 K. PL spectra were acquired at each temperature step, maintaining constant the power on the sample. All the spectra were corrected by the spectral response of the system. The measured temperature of the sample is subjected to an error of about ±5 K, associated to the different position of the sample and the sensor.

C. Electrical characterization

Measurements were done in dark conditions using an Agilent B1500 semiconductor device analyser, placing the devices in a Cascade Microtech Summit 11000 probe station, and insulating them from the external electromagnetic noise using a faraday cage. Devices defined with 1-mm Al contact diameter were employed, since they exhibited the best electrical response and reproducibility.

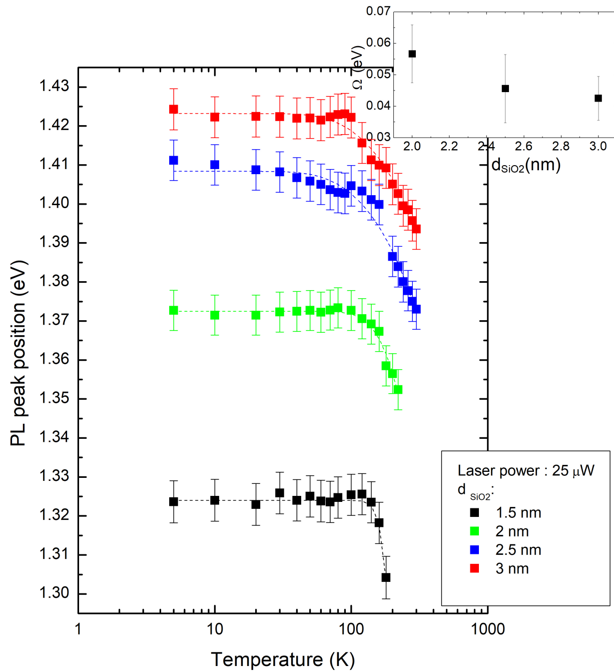

FIG. 3: PL peak energy evolution with temperature for each sample with different $d_{\mathrm{SiO_2}}$ barrier. The data shown in the image were obtained using the highest laser power, 25 μW (54 μW/cm^2). The error bars take into account both the fitting error and a systematic uncertainty from the PL spectra acquisition. The dashed lines correspond to the theoretical model expressed in EQ. (2), which properly fits the results without the necessity to exclude any data point from lower temperatures. The inset graph corresponds to the average phonon energy values obtained through the described fiting process. Average phonon energy for the sample with a barrier of 1.5 nm is not plotted due to problems with the fitting of this value.

III. RESULTS AND DISCUSSION

A. Low-temperature photoluminiscence

Temperature-dependent PL spectra for 3-nm-thick barriers sample are shown in FIG. 2. The spectra show a main broad feature centred around 850-900 nm, which is attributed to the quantum-confined emission of the band-to-band recombination of excited electron-hole pairs in Si NCs [5]. The spectra corresponding to different temperatures are plotted, which exhibit a shift PL peak position at shorter wavelengths (i.e., higher energies) at lower temperatures.

PL spectra were systematically acquired for each sample with different $d_{\mathrm{SiO_2}}$, by fixing the laser spot and scanning through the whole temperature range. From each spectrum, both PL intensity and wavelength were transformed to the energy coordinate ($E = h{\cdot}c/\lambda$, being E the photon energy, h the Planck's constant, c the speed of light in vacuum and λ the photon corresponding wavelength) and the correction from the Jacobian-transformation was introduced. These results are presented in FIG. 3. As can be seen in the graph, the thicker the SiO_2 barriers, the higher the energy, as expected from a more effcient quantum confinement of carriers at larger inter-NC distances (i.e., lower NC-NC interaction). However, we cannot rule out a possible diffusion of Si from the SRON layers towards the SiO_2 barriers, being this effect enhanced at thinner layers; this may induce the formation of larger NCs than the SRON layer thickness resulting in a loss of quantum confinement. As well, the peak energy evolution for each sample follows an increase when decreasing the temperature in the high-temperature regime, followed by a saturation below 100 K. Regarding the evolution at higher temperatures, the trend exhibits increasing slope at thinner SiO_2 barriers.

It is known that the band gap energy of bulk semiconductors increases at lower temperatures due to the thermal expansion of its lattice and electron-phonon interaction, which is described by the Varshni law [6]:

$$E_{gap}(T) = E_g(0) - \frac{\alpha{\cdot}T^2}{T+\beta}, \qquad (1)$$

where T is the temperature, $E_{\mathrm{g}}(0)$ is the band gap at T = 0 K, α is the thermal expansion coefficient and β is a parameter proportional to the Debye temperature, both being characteristic for the material under study. However, this expression is not valid for the whole temperature range due to the loss of physical significance of the two parameters at low temperatures [3]. This fact was checked by fitting the PL peak position using EQ. (1), which showed a strong divergence from the data at low temperatures. Considering the average lattice phonon energy and the effect of this interaction in the renormalization of the electronic states, Viña *et al.* proposed a correction to the band gap energy dependence of a semiconductor that allowed interpreting the data within the

low temperature regime [3]:

$$E_{\text{gap}}(T) = E_{\text{gap},0} - A\left(\frac{2}{exp\left(\frac{\Omega}{K_{\text{b}}T-1}\right)}+1\right), \qquad (2)$$

where A is a constant describing the strength of the electron-phonon interaction, K_{B} is the Boltzmann's constant and Ω is related to the average phonon energy. In contrast to EQ. (1), EQ. (2) has indeed full physical significance in practically the whole temperature range. As we can see in FIG. 3, the dotted lines correspond to the fits according to EQ. (2). From the fit we could get, for each sample, the different parameters described previously in this paragraph. Please note that we also checked that this expression is only valid for low areal power densities, since at higher power densities the deviation of the PL peak energy from the theoretical expression due to saturation effects was observed. According to the fitting values, the strength of the electron-phonon interaction and the average phonon energy increased at thinner SiO_2 barriers, as we can see for the average phonon energy in the inset of FIG. 3. In addition, we also checked that the $E_{\text{gap},0}$ well correlates to the energy extrapolation at 0 K.

The evolution of the average phonon energy with the barrier thickness, being lower for thicker barriers, can be explained as it follows. For thicker barriers, the inter-NC distance is larger, and the isolation of each NC from the interaction of their neighbours is consequently greater: therefore, quantum confinement is expected to be more efficient. This occurrence enhances the delocalization of the electron wavefunction at the minimum of the conduction band and its hole counterpart at the maximum of the valence band, which increases the probability of a quasi-direct band-to-band electron transition without the need for the participation of a lattice phonon in this process. This hypothesis is supported by our obtained average phonon energy values. It must be mentioned that the trend from the average phonon energy obtained is, as already discussed, the one expected from a physical point of view. However, the values that we get show a certain discrepancy with the ones that we found in the literature [4]. Although this is out of the scope of the present thesis, it would be of certain interest in future studies to check where this discrepancy comes from.

B. Electrical results

The study of charge transport taking place through the Si NCs was performed via the analysis of the data obtained from the current-voltage characteristics for each sample, (see FIG. 4). The $I(V)$ curves exhibit three different regimes depending on the voltage applied [7]: (I) movement of free charges already present within the sample (low electric fields), (II) generation of electron-hole pairs within the defects of the SiO_2 matrix or at the Si NC/SiO_2 interface due to the electric field (medium fields), and (III) net charge injection through the aluminium electrode (high electric fields). This last region was found to well fit to a mechanism of Fowler-Nordheim (F-N) injection. This regime is characterized by $q{\cdot}\phi_{\text{b}}$, known as the band offset energy at the electrode/dielectric interface. This value quantifies the injection probability, i.e., the quantum mechanical probability that injected electrons from the metal electrode are transmitted through the dielectric (in this case, the Si NC superlattices). The current obtained in this condition can be expressed as:

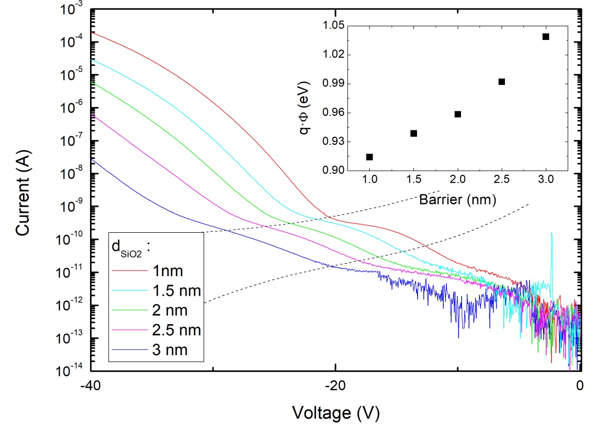

FIG. 4: $I(V)$ characteristics from the devices under study. The dashed lines are just a guide to the eyes to observe the different transport regimes described in the text. The inset graph plots the evolution of the band offset energy obtained from fitting the high electric field regime (F-N charge transport mechanism) from each curve through the EQ. (3).

$$I_{\text{FN}}(V) = \frac{Sq^2}{8\pi h\phi_{\text{b}}}\frac{V^2}{d^2}exp\left(-\frac{8\pi\sqrt{2qm^*}}{3h(V/d)}\phi_b^{\frac{3}{2}}\right), \qquad (3)$$

being S the device area, m^* the carrier effective mass and d dielectric thickness to be overcomed by the carrier. Using the data from the F-N region (region III), we can fit the different obtained curves using EQ. (3). This process is not direct and some mathematical manipulation is needed in order to transform the data from the F-N region into a straight line, then the fitting process using EQ.(3) can be immediately done. The results for the band offset energy released from the fits are plotted in the inset in FIG. 4. The obtained band offset energy values are the ones expected from the literature [8]. As it can be observed, the energy offset increases at thicker SiO_2 barriers. This result is indeed not surprising, since a dielectric layer with an increasing thickness will pose a higher resistance to charge transport, and a consequent reduction of conductivity, as has been quantified by the effective band offset energy.

IV. CONCLUSIONS

We have studied the temperature-dependent PL emission and electrical properties of different Si NC superlattice samples with a constant Si NC size and varying the thickness of the SiO_2 layer, from 1 nm to 3 nm with steps of 0.5 nm. From the measurement of the PL properties under low temperature conditions we were able to obtain the value of the average phonon energy as a function of the barrier thickness, which confirms that thicker barriers enhance the quantum confinement of Si NCs. For the electrical properties, the offset band energy for each sample was obtained after fitting the high electric field regime of the $I(V)$ curves with a F-N-type charge transport mechanism. The increase of this value at thicker SiO_2 barriers is in agreement with a reduction of the conductivity in our samples. Overall, it has been proved in this work that a better isolation of the Si NCs improves the quantum confinement and therefore enhances the optical properties of Si, but at the expense of the electrical conductivity.

Acknowledgments

First of all, I would like to thank Dr. Julià López Vidrier for his constant assistance and advice. Also I am really grateful to him of making my internship in Freiburg pleasant and full of knowledge. In addition, I would like to thank to the full nanotechnology group at IMTEK that made me feel as one more component of the team. Also I would like to thank to Dr. Sergi Hernández Márquez who has helped me a lot during all the writing process. Last but not least, I would like to give thanks to all my family and friends for the constant support during all this process.

[1] L. T. Canham, Appl. Phys. Lett. 57, 1046 (1990).

[2] M. Zacharias, J. Heitmann, R. Scholz, U. Kahler, M. Schmidt, and J. Bläsing, Appl.Phys. Lett. 80, 661 (2002)

[3] L. Viña, S. Logothetidis, and M. Cardona, Phys. Rev. B30, 1979 (1984).

[4] A. M. Hartel, S. Gutsch, D. Hiller, and M. Zacharias, Phy. Rev. B85, 165306 (2012)

[5] J. López-Vidrier, S. Hernández, D. Hiller, S. Gutsch, L. López-Conesa, S. Estradé, F. Peiró, M. Zacharias, and B. Garrido, J. Appl. Phys. 116, 133505 (2014)

[6] Y. P. Varshni, Physica 34, 149 (1967).

[7] S. Gutsch, J. Laube, A. M. Hartel, D. Hiller, N. Zakharov, P. Werner, and M. Zacharias, J. Appl. Phys. 113, 133703 (2013).

[8] M. Scnabel, M. Canino, S. Künhold-Pospischil, J. López-Vidrier, T. Klugermann, C. Weiss, L. López-Conesa, M. Zschintzsch-Dias, C. Summonte, P. Löper, S. Janz, and P. R. Wilshaw, Phy. Rev. B91, 195317 (2015).